# Electrodeposition of Cu onto Reconstructed Pt(100) and Pt(110) Surfaces

By M. S. Zei and G. Ertl

Fritz-Haber-Institut der Max-Planck-Gesellschaft,
Faradayweg 4−6, D-14195 Berlin, Germany

(Received January 16, 1996)

*Adsorption / Electrochemistry / Electron diffraction*

The structural properties of reconstructed Pt(100) and (110) surfaces in $H_2SO_4$ solution and after underpotential deposition (UPD) of Cu were investigated by means of LEED, RHEED, Auger electron spectroscopy and voltammetry. Potential cycling between −0.2 and +0.2 V leaves the surface reconstructions unaffected. While with Pt(110) the 1×2 surface periodicity survives Cu UPD as well as subsequent stripping, with Pt(100) the surface reconstruction is lifted by Cu UPD. Structural models for Pt(110) covered by 1 and 2 monolayers (ML) of Cu are presented which are consistent with the various experimental observations. Specific adsorption of anions ($SO_4^{2-}$ and Br⁻) on Cu/Pt(110) causes the formation of ordered overlayers under certain conditions.

## 1. Introduction

The structural properties of reconstructed electrode surfaces have so far been mainly investigated for gold [1−3]. Although platinum is of importance for electrocatalysis, relatively few studies have been reported in the literature, presumably because of the problems encountered with preparation and handling of well-defined surfaces in electrochemical environments. It was recently found that the reconstructed Pt(100)hex-surface may be stable in an electrochemical cell which is in contrast to previous reports [5−7]. Likewise the Pt(110)-1×2 surface was reported to be stable in sulfuric acid over the double layer charging region [8, 9], while in a recent STM study it was concluded that the missing row structure of this plane is lifted upon immersion into the electrolyte [10].

Underpotential deposition of Cu has, on the other hand, again been extensively studied with Au electrodes [11−17], while relatively few studies with Pt were published [9, 10, 18−20]. For Pt(110) it was reported that the

$1 \times 2$-reconstruction is stable up to $\Theta_{Cu} = 0.5$ while beyond that coverage the reconstruction is lifted [9, 18]. After stripping and emersion at 0.6 V the $1 \times 2$-structure was still found to exist [9].

The overall situation for the Pt(100) and (110) surfaces appears still rather unclear, and hence a systematic study of these systems was performed. Structural properties were probed by *ex situ* LEED/RHEED studies which were supplemented by AES and voltammetry. Apart from the stability of the reconstructed Pt(100) and (110) surfaces under the influence of potential cycling in $H_2SO_4$ solution, also the structure of Pt(110) with Cu UPD in $SO_4^{2-}$, $Cl^-$ and $Br^-$ containing solutions was investigated. Among others, it will be concluded that the Cu coverages on Pt(110) derived from coulometry, AES and LEED data are quite at variance to previously reported results [9, 21−23].

## 2. Experimental

The experimental set-up includes a UHV system equipped by LEED, RHEED and AES facilities, an electrochemical cell and a closed sample-transfer [24]. The single crystal samples were discs of 8 mm diameter and 2 mm thickness which were mounted between tantalum wires which also served for resistive heating. The samples were subject to prolonged cycles of sputtering (30 min at $5 \times 10^{-5}$ Torr Ar, 600 °C) and annealing (900 °C) until AES and LEED/RHEED indicated the formation of clean and well-ordered surfaces. The electrolyte solutions were prepared from $H_2SO_4$, HCl, NaBr (Merck, suprapure) and $CuSO_4$ (Merck, p.a.), respectively, and triply distilled water. All potentials are referred to a Ag/AgCl/KCl (sat.) reference electrode.

## 3. Results and discussion

Figs. 1 and 2 display the RHEED and LEED patterns from the clean Pt(100) and Pt(110) surfaces, respectively, whereby the absence of noticeable impurity concentrations (apart from small amounts of carbon) had been checked by AES. Diffraction features characteristic for the reconstructed 'hex'-$(5 \times 20)$-Pt(100) and $(1 \times 2)$-Pt(110) surfaces are clearly discernible. The electrodes were subsequently transferred into the electrochemical chamber (which was backfilled by 5N Ar) and immersed into the electrolyte where cyclic voltammograms could be recorded. After emersion the electrochemical chamber was evacuated and the sample transferred back into the UHV chamber for surface characterization. As reported before [4], the reconstructed Pt(100) surface remains stable in contact with a sulfuric acid solution. As confirmed in the present work this holds even after 8 potential cycles between $-0.2$ and $+0.35$ V. This becomes evident from inspection
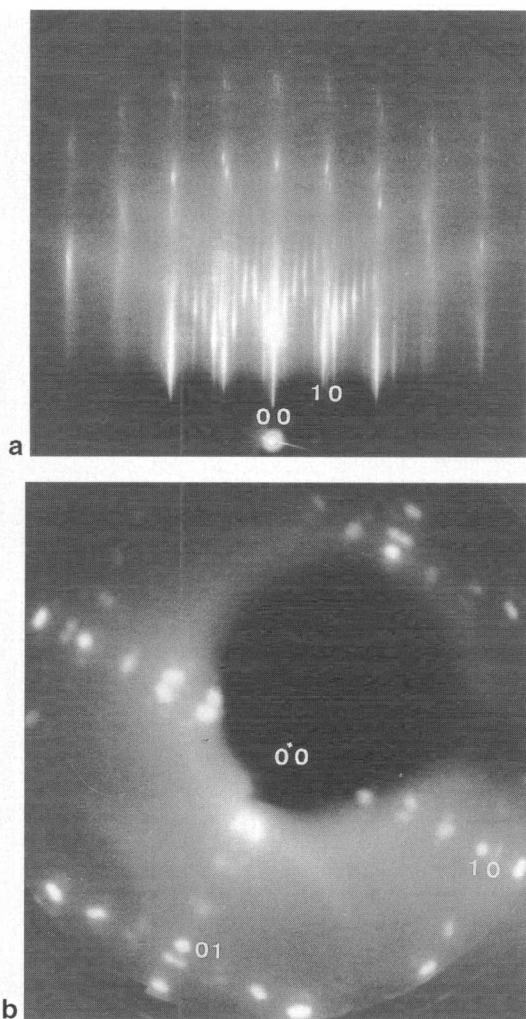
**Fig. 1.** a) RHEED (⟨110⟩azimuth, 40 keV) and b) LEED (50 eV) patterns from the reconstructed 'hex'-Pt(100) surface, after preparation by sputtering and annealing in the UHV chamber.

of the RHEED pattern in Fig. 3a which was recorded after emersion at 0 V, where an additional streak between the (00) and (21) substrate reflections characteristic for the hex-structure is descernible. For comparison Fig. 3b shows a pattern from an unreconstructed Pt(100)-surface where these features are absent. The latter sample was prepared in UHV by sputtering and annealing and kept in a vacuum of $3 \times 10^{-10}$ Torr for 6 days, which treat-
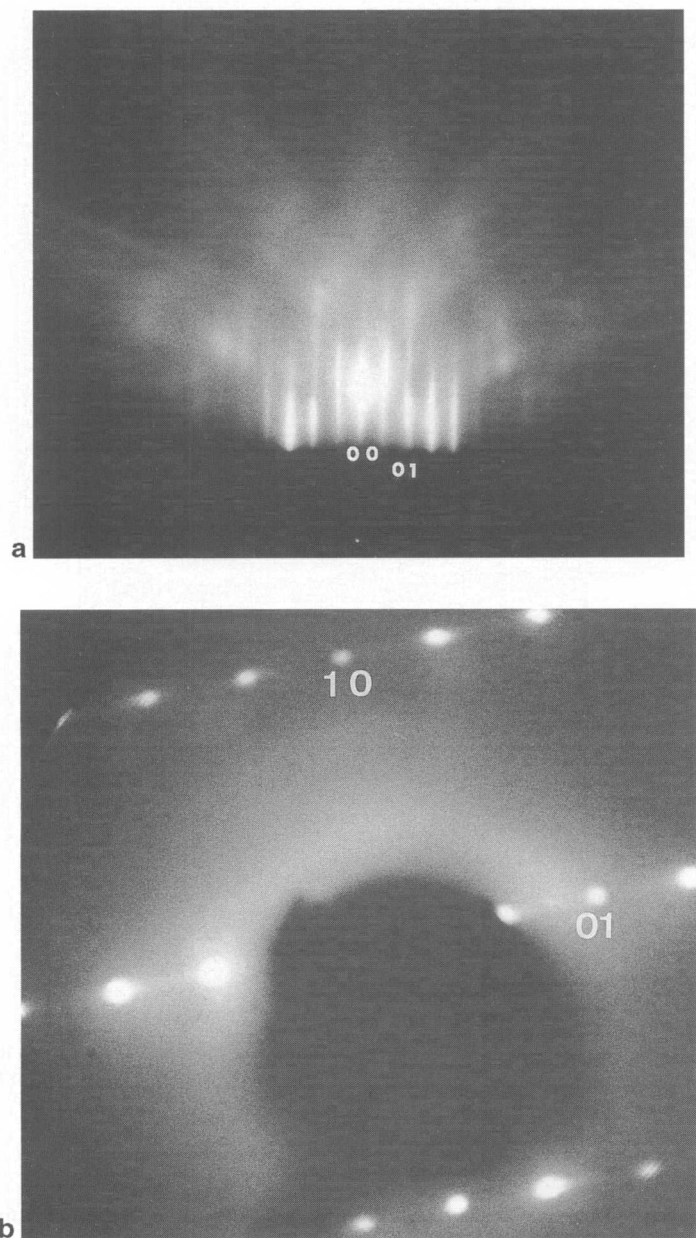
**Fig. 2.** a) RHEED ((110)azimuth, 40 keV) and b) LEED (50 eV) patterns from the clean 1×2-Pt(110) surface.

($\bar{2}\bar{1}$)          (00)          (21)
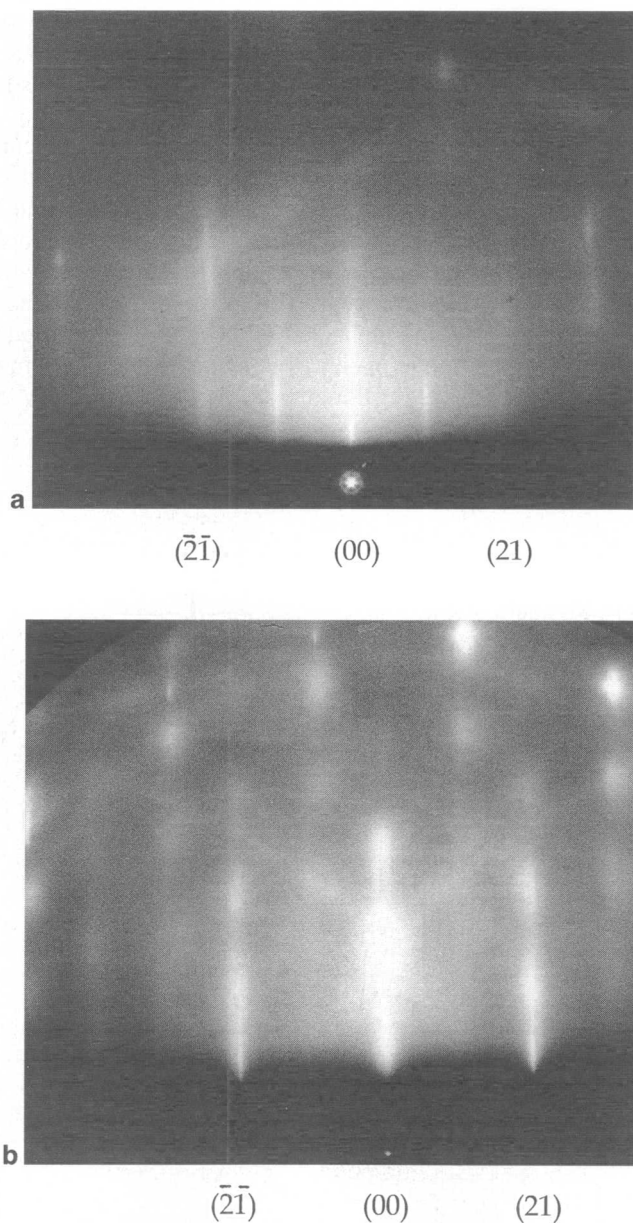
**Fig. 3.** RHEED patterns (⟨031⟩azimuth) from Pt(100) electrodes. a) After potential cycling in H₂SO₄ solution the 'extra' reflections between the (00) and (21) beams indicate that the hex-reconstruction is still present. b) After residual gas adsorption these diffraction features are absent because the reconstruction has been lifted.

ment obviously enabled lifting of the reconstruction by adsorption from the residual gas atmosphere. Quite in contrast, a reconstructed $1 \times 2$-Pt(110) surface was observed to remain stable under identical conditions for at least 2 months.

The $(1 \times 2)$-Pt(110) sample exhibits in 0.01 M $H_2SO_4$ current-potential data similar to those reported previously by Michaelis and Kolb [9]. Emersion after potential cycling between $-0.2$ and $+0.2$ V and transfer to the UHV chamber led to the observation of diffraction patterns in which the $1 \times 2$-reconstruction was still clearly discernible, in agreement with previous reports [8, 9]. However, quite recently Beitel *et al.* [10] claimed that the $1 \times 2$-reconstruction of a flame annealed Pt(110) surface is lifted upon immersion into $H_2SO_4$-solution at open cell potential. Most likely in this study the initial state of the surface differed from the stringent UHV conditions employed in the present work.
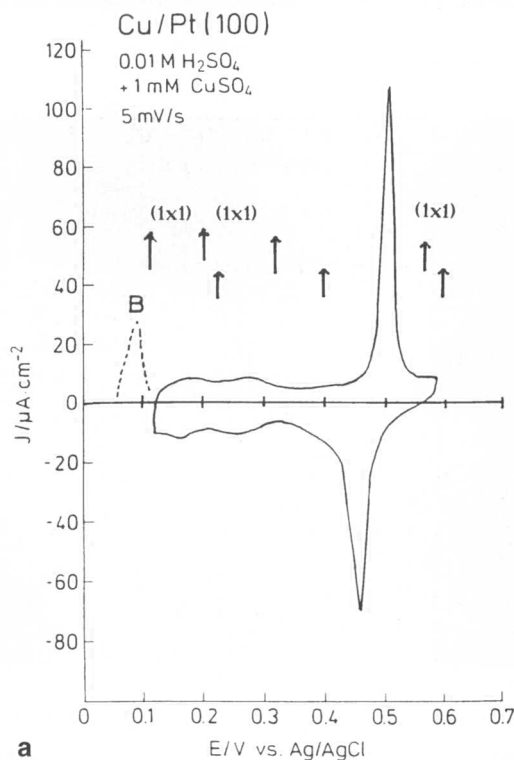


**Fig. 4.** Cyclic current-potential curves for the underpotential deposition (UPD) of Cu on Pt electrodes. a) Pt(100) in $10^{-2}$ M $H_2SO_4 + 10^{-3}$ M $CuSO_4$, scan rate 5 mV/s. b) Pt(110) in $10^{-2}$ M $H_2SO_4 + 10^{-3}$ M $CuSO_4$, 10 mV/s. c) Pt(110) in $10^{-2}$ M $H_2SO_4 + 10^{-3}$ M $CuSO_4 + 10^{-4}$ M HCl, 10 mV/s. B: Potential for bulk metal deposition.
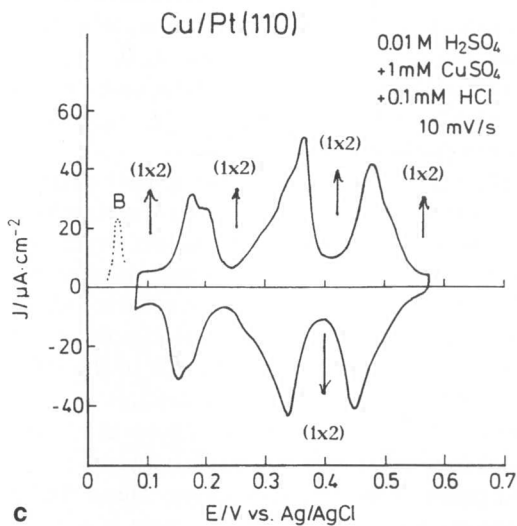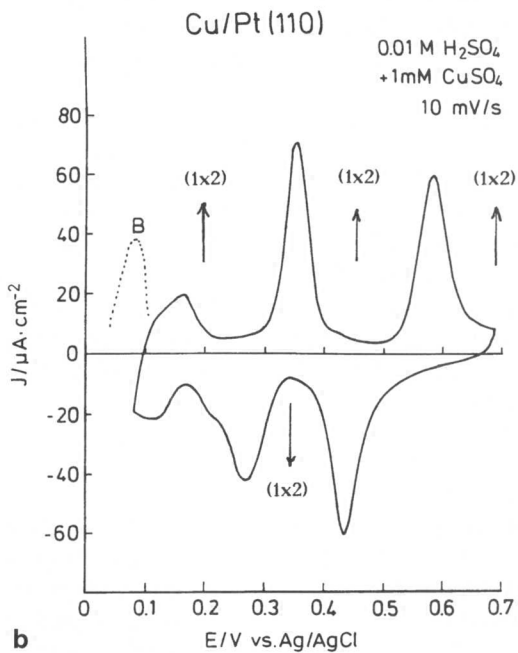
**Fig. 4.** Continuation.

**Table 1.** Comparison of AES peak ratios and corresponding Cu coverages with the coulometric data obtained from different labs.

| Cu/Pt(110) | $Q$ ($\mu$C/cm$^2$) | $I_{Cu}/I_{Pt}$ | $\Theta_{Cu}$ (ML) | Reference | Solutions |
|---|---|---|---|---|---|
| | 514 | | 1.74 | [18] | 0.1 M HClO$_4$ +5 mM Cu(ClO$_4$)$_2$ |
| | 504 | | 1.71 | [22] | +0.5 M H$_2$SO$_4$ +1 mM CuSO$_4$ |
| | 310 | | 1.05 | [21] | +0.5 M H$_2$SO$_4$ +1 mM CuSO$_4$ |
| | 600 | 1.2+0.1 | 2.0 | a | +0.01 M H$_2$SO$_4$ +1 mM CuSO$_4$ |
| | 533 | 1.2+0.1 | 1.8 | a | +0.1 mM HCl |
| | 562 | 1.2+0.1 | 1.9 | a | +0.1 mM NaBr |

a  Present results.

The electrosorption of Cu was performed in solutions containing $10^{-2}$ M H$_2$SO$_4$ + $10^{-3}$ M CuSO$_4$. The cyclic voltammogram for Pt(100) is shown in Fig. 4a and is in qualitative agreement with previous reports [21, 22] in that it exhibits essentially a single pronounced peak. By contrast, the data for Pt(110) as reproduced in Fig. 4b exhibits *two* current peaks, each one associated with a charge of about 300 $\mu$C/cm$^2$ corresponding to 1 monolayer (ML) of Cu. This conclusion is in agreement with the results from analysis of Auger electron spectroscopy measurements. The latter was based on determination of the Auger peak ratio $I_{Cu}/I_{Pt}$ which was calibrated through 1 ML of Cu deposited onto a Pt(100) surface. The data resulting for Pt(110) are listed in Table 1 and are in fair agreement with previous results by Aberdam *et al.* [18].

The LEED pattern from Pt(100) shows a 1×1-periodicity after deposition of 1 ML Cu which indicates that the reconstruction has been lifted and that the Cu atoms form a pseudomorphic overlayer. On the other hand, the Pt(110) surface still exhibits a (1×2)-pattern after emersion from the whole potential range for Cu deposition. The relative intensities of the half-order spots, however, vary and indicate differences of the actual surface structures. Their intensity is comparable to that of the integer order reflections for the Cu-free surface (emersion at potentials ≥+0.56 eV) as well as for the completely Cu-covered surface (emersion at ∼+0.2 V), while they are only very faint for emersion at potentials between ∼+0.4 and 0.5 V, i.e. between the two peaks of the voltammogram. These findings are partly in disagreement with previous reports [9, 18] where it was concluded that the 1×2-periodicity is gradually removed with progressing Cu deposition. In order to obtain additional information about the factors determining the 1×2-superlattice on Pt(110) Cu UPD experiments in different solutions

**Table 2.** Summary of intensity ratio ($I(0,1/2)/I(0,1)$) of a ($1 \times 2$) LEED patterns for Cu UPD on Pt(110)-($1 \times 2$) surface as a function of copper and coadsorbate coverages in different electrolytes.

| Electrolyte | Emersion potential | $\Theta_{Cu}$(AES) (ML) | $\Theta$(charge) ($\mu C/cm^2$) | $\Theta_{SO_4}$ | $\Theta_{Cl}$ | $\Theta_{Br}$ | $I(0,1/2)/$ $I(0,1)$ |
|---|---|---|---|---|---|---|---|
| 1 mM CuSO$_4$ | +0.45 V(I) | 1 | 300 | 0.2 | – | – | 0.1 |
| +0.01 M H$_2$SO$_4$ | +0.2 (II) | 2 | 600 | 0.3 | – | – | 1 |
| +0.1 mM HCl | I | 1 | 300 | 0.1 | 0.1 | – | 0.1 |
| | II | 2 | 600 | 0.2 | 0.15 | – | 1 |
| +0.1 mM NaBr | I | 1 | 300 | – | – | 0.2 | 0.1 |
| | II | 2 | 600 | – | – | 0.5 | 1 |

295 $\mu C/cm^2$ = 1 ML Cu on Pt(110)-($1 \times 1$) surface

$I(0,1/2)/I(0,1)$ = intensity ratio of the half-order to integral-order beam of ($1 \times 2$) LEED pattern

were performed. The coulometric and structural data are summarized in Table 2. The voltammogram in a solution containing, in addition, $10^{-4}$ M HCl is reproduced in Fig. 4c. It exhibits essentially the same features as the chloride-free solution (Fig. 4b), and also the diffraction data are quite similar. The LEED intensity ratio of half-order and integral spots is about unity for the Cu-free as well as Cu-saturated (2 ML) surface, while it is only about 0.1 if emersion was made at +0.45 V where only 1 ML Cu was left on the surface. These findings indicate that the surface structure is not noticeably affected by specific adsorption of anions. This conclusion is supported by AES measurements which revealed that the Cl$^-$ and SO$_4^{2-}$ concentrations never exceeded 0.1 and 0.2 ML, respectively, irrespective of the emersion potential. Practically identical results were obtained if Br$^-$ ions were added to the sulfuric acid solution.

These results are somewhat surprising if compared with corresponding observations with Au electrodes: While the $1 \times 2$-Pt(110) surface is obviously stable, even in solutions containing halogenide ions, up to potentials of $\sim +0.6$ V, with Au(110) the reconstruction is lifted around +0.2 V [26], while for Au(100) the potential for the ($5 \times 20$) $\rightarrow$ ($1 \times 1$) transition is shifted from +0.4 to +0.2 by specific adsorption of Cl$^-$ [27]. Presumably the reconstructed Pt surfaces exhibit a higher thermodynamic stability than the corresponding Au planes. Apart from this the surface mobility of Pt atoms is much lower than that of Au atoms as demonstrated by STM experiments in electrolyte solutions [25, 26, 28, 29]. In order to rule out any effect of specifically adsorbed anions on the observed surface structural data, the samples were thoroughly rinsed with triply distilled water after emersion at the various potentials. Subsequently recorded Auger spectra showed no

impurities apart from small amounts of carbon, while the diffraction data remained unchanged. Hence the LEED (and RHEED) patterns are merely caused by the presence of the Cu overlayers for which now structural models will be presented which can be reconciled with the intensity data on the basis of kinematic calculations of the structure factor.

The coulometric measurements as well as the Auger data convincingly demonstrated that with the $(1 \times 2)$-Pt(110) surface the saturation coverage for Cu UPD corresponds to 2 ML, whereby the coverage (ML) is defined as the ratio of density of Cu adatoms over that of Pt atoms in the topmost layer of the *non-reconstructed* (110) surface. This result is at variance with the findings of previous work [21, 23] where on completion of just 1 ML was concluded. However, such a result would be hard to rationalize even for a non-reconstructed (110) surface: In contrast to the more densely-packed (non-reconstructed) (111) and (100) planes on which deposition of
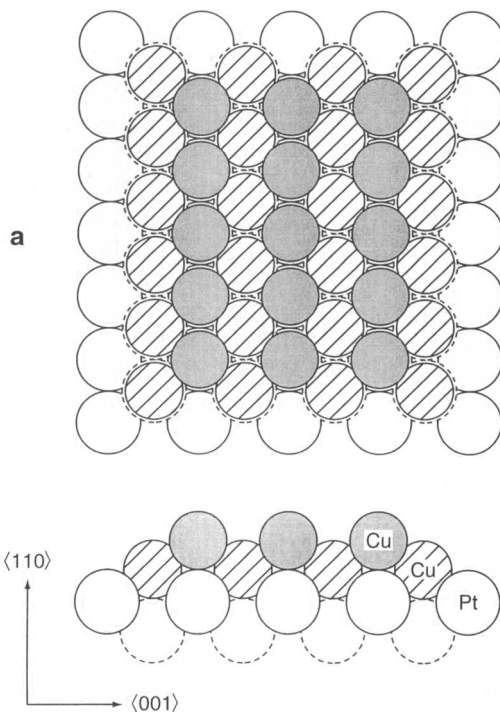


**Fig. 5.** Structure models for Cu overlayers on Pt(110). a) Hypothetical structure model for 2 ML of Cu deposited onto a non-reconstructed Pt(110) surface. b) Structure model and resulting LEED pattern for 1 ML Cu on the $(1 \times 2)$-Pt(110) surface. c) Structure model and resulting LEED pattern for 2 ML Cu deposited on the $(1 \times 2)$-Pt(110) surface, whereby the UPD is completed.
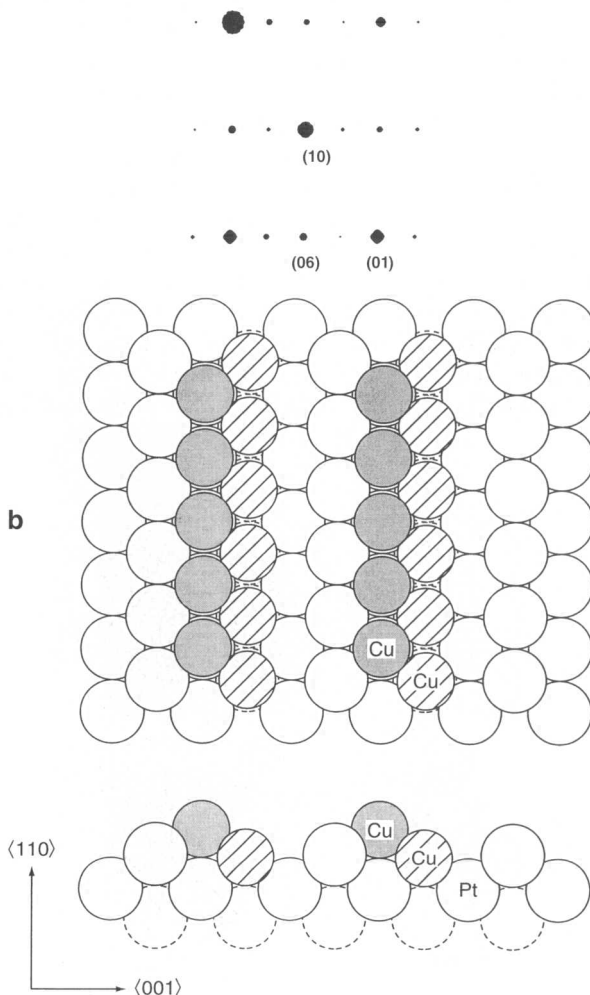
**Fig. 5.** Continuation.

1 ML leads to formation of a densely packed flat overlayer, with the more open (110) plane deposition of 1 ML would not completely suppress exposure of the Pt atoms. This would only be achieved by deposition of a second monolayer (with different bond properties) as sketched by Fig. 5a.

Accordingly with the reconstructed $(1 \times 2)$-Pt(110) surface we may construct structure models with 1 ML and 2 ML Cu, respectively, in which the Cu atoms form parallel rows along the $[1\bar{1}0]$-direction until no Pt atoms are exposed any more to the electrolyte (Figs. 5b and c). The corrugation with
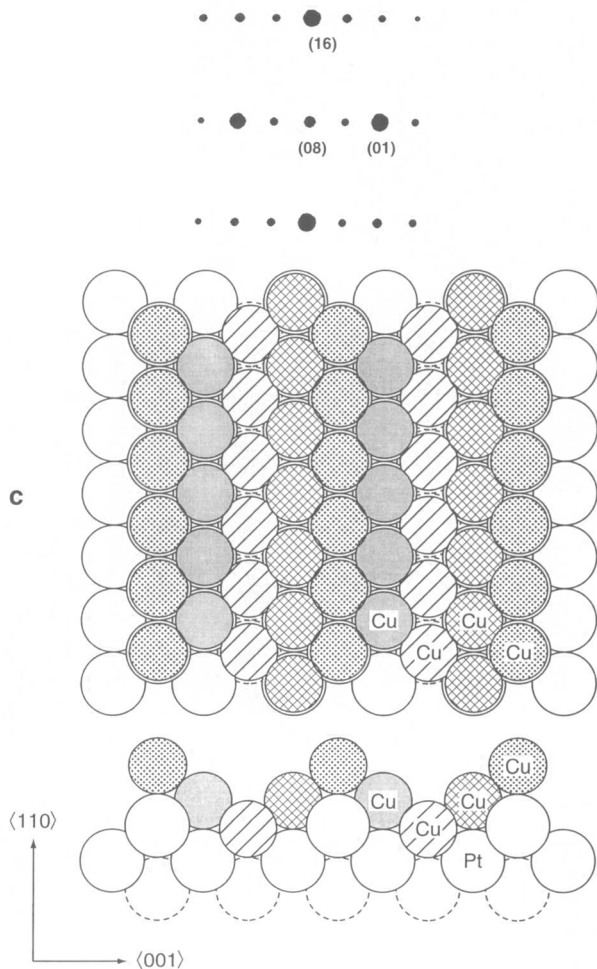
**Fig. 5.** Continuation.

$(1 \times 2)$-periodicity is considerably stronger with the 2 ML-structure (Fig. 5c) than with the 1 ML-phase (Fig. 5b). Consequently the intensities of the half-order diffraction beams are expected to be much higher for the former than for the latter phase which is confirmed by kinematic calculations and is in agreement with the experimental evidence presented above.

Finally two superstructures formed by specific adsorption of anions will be presented. If the Pt(110) electrode is emersed from a $Cu_2SO_4 + H_2SO_4$ solution at a potential of $+0.45$ V, i.e. between the two current peaks of the voltammogram where the surface is covered by 1 ML Cu, the LEED pattern
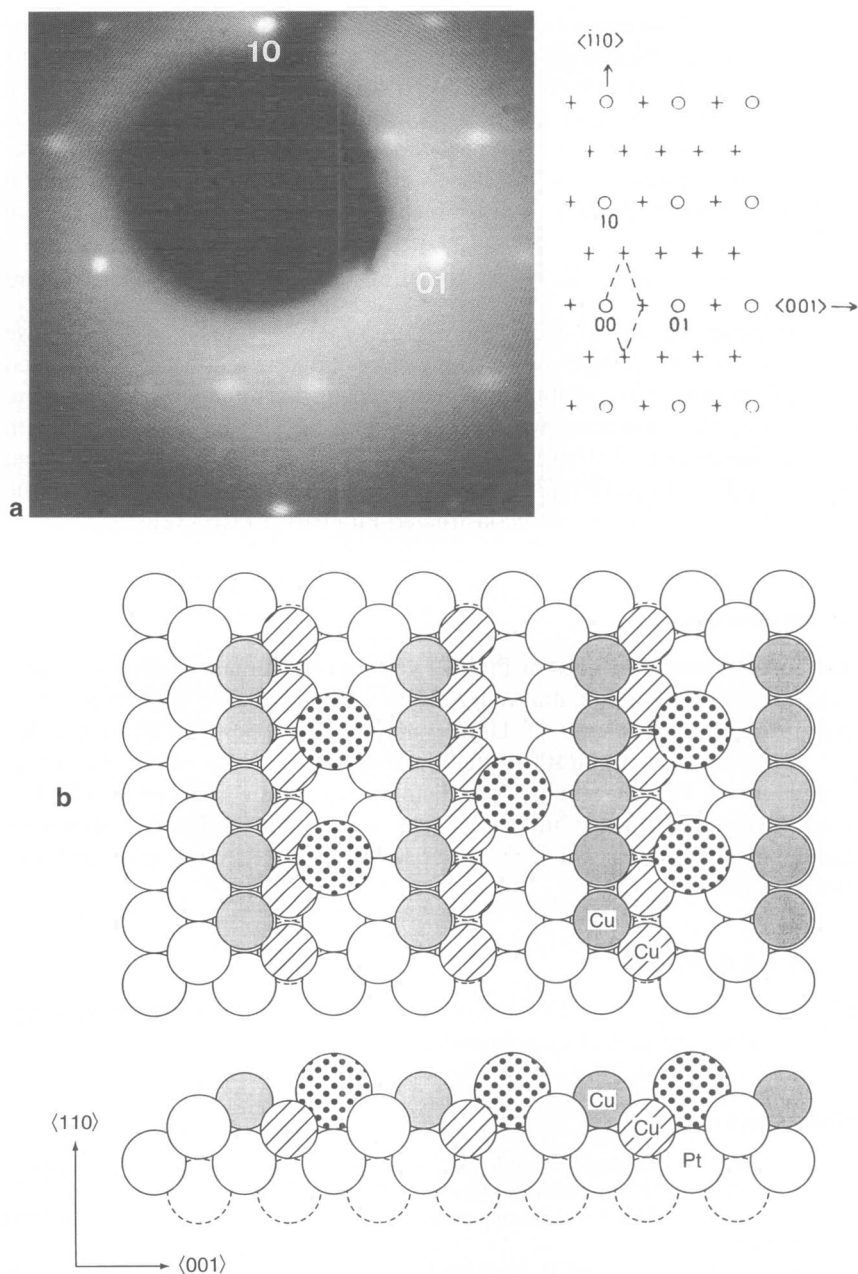
**Fig. 6.** a) Sketch of the c(2×4)-LEED pattern observed from the (1×2)-Pt(110) electrode after deposition of 1 ML Cu in $H_2SO_4$ solution and subsequent emersion at +0.4 V. b) Structure model for the ordered c(2×4)-overlayer formed by adsorbed $SO_4^-$ ions.

exhibits a c(2×4)-superstructure as sketched in Fig. 6a which has to be attributed to an ordered overlayer of $SO_4^{2-}$ ions. At other potential regions it does not form an ordered structure. The same type of pattern had been observed with sulfate adsorption on a clean Au(110) surface [30] as well as on a non-reconstructed Pt(110) surface [9]. A structure model for the present system is presented in Fig. 6b. Its coverage (0.25 ML) is in agreement with the value (0.2 ML) derived from AES measurements as listed in Table 2.

In the presence of $Br^-$ ions sometimes a $\begin{pmatrix} 0.73 & 1 \\ 0.73 & -1 \end{pmatrix}$ superstructure superimposed on the (1×2)-pattern was observed, presumably on those parts which were subject to wet emersion. Auger spectroscopy indicated that sulfate ions were completely displaced by bromine ions. A structure model may be constructed which consists of a densely packed adlayer with Br−Br distances of 3.9±0.1 Å, similarly as with the 7×7 structure formed on the Cu/Pt(111) surface [31]. It differs, however, from the structure of the Br-adlayer formed on an unreconstructed Pt(110)-surface [32].

# 4. Summary

The reconstructed surfaces of Pt(100) and Pt(110) remain stable in sulfuric acid solution over a potential range from −0.2 to +0.2 V with respect to a Ag/AgCl-reference electrode. Underpotential deposition (UPD) of Cu lifts the reconstruction of Pt(100) after deposition of 1 ML, while the 1×2-periodicity of Pt(110) persists. Two distinct states with 1 ML and 2 ML Cu, respectively, are formed in the latter case for which plausible structural models are presented which are compatible with the coulometric and diffraction data.

### References

1. D. M. Kolb, G. Lehmpfuhl and M. S. Zei, J. Electroanal. Chem. **179** (1984) 289.
2. D. M. Kolb and J. Schneider, Surface Sci. **162** (1985) 764.
3. B. M. Ocko, J. Wang, A. Davenport and H. S. Isaacs, Phys. Rev. Lett. **65** (1990) 1466.
4. M. S. Zei, N. Battina and D. M. Kolb, Surface Sci. Lett. **309** (1994) L519.
5. F. T. Wagner and P. N. Ross, Jr., J. Electroanal. Chem. **150** (1983) 141.
6. R. M. Ishikawa and A. T. Hubbard, J. Electroanal. Chem. **69** (1976) 317.
7. F. T. Wagner and P. N. Ross, Jr., Surface Sci. **160** (1985) 305.
8. A. S. Homa, E. Yeager and B. D. Cahan, J. Electroanal. Chem. **150** (1983) 181.

9. R. Michaelis and D. M. Kolb, J. Electroanal. Chem. **328** (1992) 341.
10. G. Beitel, O. M. Magnussen and R. J. Behm, Surface Sci. **336** (1995) 19.
11. H. O. Beckmann, H. Gerischer, D. M. Kolb and G. Lehmpfuhl, Symp. Faraday Soc. **12** (1977) 51.
12. P. N. Ross, Jr., Surface Sci. **102** (1981) 463.
13. Y. Nakai, M. S. Zei, D. M. Kolb and G. Lehmpfuhl, Ber. Bunsenges. Phys. Chem. **88** (1984) 340.
14. O. R. Melroy, M. G. Samant, G. L. Borges, J. G. Gordon, L. Blum, J. H. White, M. J. Albarelli, M. McMillan and H. D. Abruna, Langmuir **4** (1988) 728.
15. O. M. Magnussen, J. Hotlos, R. J. Nichols, D. M. Kolb and R. J. Behm, Phys. Rev. **64** (1990) 2929.
16. F. A. Möller, O. M. Magnussen and R. J. Behm, Phys. Rev. **B51** (1995) 2484.
17. R. Michaelis, Ph.D. thesis, Free University Berlin 1991.
18. D. Aberdam, R. Durand, R. Fauré and F. El-Omar, Surface Sci. **162** (1985) 782.
19. K. Shashibata, N. Furya and K. Itaya, J. Electroanal. Chem. **316** (1991) 361.
20. T. Abe, G. M. Swain, K. Shashikata and K. Iaya, J. Electroanal. Chem. **382** (1995) 73.
21. D. M. Kolb, R. Kötz and K. Yamamoto, Surface Sci. **87** (1979) 20.
22. C. L. Scortichini and C. N. Reilley, J. Electroanal. Chem. **139** (1982) 233; 247.
23. J. W. Schultze and D. Dickertmann, Surface Sci. **54** (1976) 489.
24. D. M. Kolb, G. Lehmpfuhl and M. S. Zei, *NATO-ASI Series C. Spectroscopic and Diffraction Techniques in Interfacial Electrochemistry*, Kluwer Acad. Publishers 1990.
25. K. Sashikata, N. Furuya and K. Itaya, J. Vac. Sci. Technol. **B9** (1991) 457.
26. R. J. Nichols, O. M. Magnussen, J. Hotlos, T. Twomey, R. J. Behm and D. M. Kolb, J. Electroanal. Chem. **290** (1990) 21.
27. D. M. Kolb and J. Schneider, Electrochim. Acta **31** (1986) 929.
28. Y. Gao, A. Hamelin and M. J. Weaver, Phys. Rev. Lett. **67** (1981) 618.
29. O. M. Magnussen, J. Wiechers and R. J. Behm, Surface Sci. **289** (1993) 139.
30. M. S. Zei and D. Weick, Surface Sci. **208** (1989) 425.
31. R. Michaelis, M. S. Zei, R. S. Zhai and D. M. Kolb, J. Electroanal. Chem. **339** (1992) 299.
32. A. M. Bittner, J. Wintterlin, B. Beran and G. Ertl, Surface Sci. **335** (1995) 291.